Theoretical Study of Symmetric and Antysymmetric Plasmons in Chains of Coupled Plasma Cylinders

Nadiia Stognii, Nataliya Sakhnenko
Department of Higher Mathematics
Kharkiv National University of Radio Electronics (KNURE)
Kharkiv, Ukraine
e-mail: nstognii@gmail.com

Abstract—Theoretical study of plasmon resonant eigenfrequencies in coupled plasma cylinders is presented. Mechanism of the plasmonic mode coupling that can be considered as symmetric and antisymmetric combinations of isolated cylinders plasmons is investigated. Accurate analysis of the spectrum of different plasmon resonances is presented.

Keywords-plasma; surface plasmons; plasmon resonances; eigenfrequency

I. INTRODUCTION

Metallic nanostructures are the subject of growing interest in recent years due to the possibility of a strong light localization beyond the diffraction limit via the excitation of surface and local plasmons [1-2]. Various elements such as plasmonic waveguides [3-4], subwavelength resonators [5-6] and optical nanoantennas [7-9] have been studied recently. Surface and localized plasmons have been explored for their potential in single molecule detection including use of the Surface Enhanced Raman Scattering (SERS) effect [10-11], transmissions through the subwavelength apertures [12-13], subwavelength imaging [14] etc. Plasmonic structures of different shapes (nanowires, nanorods, nanospheres, nanoshells) can be produced by various fabrication techniques. The silver nanowire structure is a candidate for key components in future ultra-compact photonic devises [15]. It can be considered as a plasmon biosensor to monitor tiny biomolecular interactions [16] and as a novel modulator to control the intensity of the transmitted surface plasmon polaritons through a nanowire array [17]. Possible future nanophotonic technologies demand devices that can generate stimulated emission through the excitation of the surface plasmons [18-19]. For these applications an accurate frequency domain modeling that provides a valuable insight into fundamental processes is of great importance.

II. PROBLEM FORMULATION AND METHOD OF SOLUTION

In this paper we solve the eigenvalues problem for a chain of coupled plasma cylinders (columns). Radius of each column is a, separation distance between them is d and plasma is described by the permittivity ε_p that is given by the Drude model:

$$\varepsilon_p(\omega) = 1 - \omega_p^2 \cdot (\omega(\omega + i\gamma))^{-1} \qquad (1)$$

Here ω_p represents the plasma frequency, γ is the material absorption. Sub-wavelength resonances are possible when $\varepsilon(\omega) < 0$ (or equivalently $\omega_p > \omega$), they are called plasmon resonances or surface plasmons. The ambient medium is free space. H-polarized fields are considered. We present the z-component of the internal field as

$$H(\rho_l, \varphi_l) = \sum_{s=-\infty}^{+\infty} K_s^{(l)} J_s(k_p \rho_l) e^{is\varphi_l} \qquad (2)$$

and the external field as

$$H(\rho_l, \varphi_l) = \sum_{l=1}^{N} \sum_{s=-\infty}^{+\infty} M_s^{(l)} H_s^{(2)}(k\rho_l) e^{is\varphi_l} \qquad (3)$$

Here (ρ_l, φ_l) are set of N polar systems of coordinates, associated with each cylindrical columns ($l = 1...N$), $z-$axis is parallel to the cylinders, $k = \omega \cdot c^{-1}$, $k_p = n_p \omega c^{-1}$, c is light velocity in a vacuum, $n_p = \sqrt{\varepsilon_p(\omega)}$, $\varepsilon_p(\omega)$ is defined by formula (1), time dependence is $e^{i\omega t}$.

Unknown coefficients K_s and M_s are found from the boundary conditions, requiring the continuity of the tangential components of the total electric and magnetic fields at each cylindrical column's surface. Using the addition theorem for the Bessel functions we arrive to an infinite system of algebraic equations that can be truncated in order to provide a controlled numerical precision. We have to mention that all eigenfrequencies are complex $\omega = \omega' + i\omega''$, where $\omega'' < 0$ represents damping and ω' is associated with the eigen oscillation frequencies. Quality (Q) factor of plasmons can be evaluated through the formula $Q = \omega'/2\omega''$.

III. RESULTS

Eigenvalue problem in an isolated plasma cylinder is treated analytically. Figure 1 illustrates the value of the real part of plasmon eigenfrequency versus normalized frequency (ka) for different values of $w_p = \omega_p a c^{-1}$, that we will call further a normalized plasma frequency. We have to stress that

there is no solution for the case $s=0$ (s is a numbers of angular field variations). It is seen that plasmon resonances for different values of s are closely spaced. Field portraits of the plasmons are shown in the inset of Fig. 1 (upper left-hand corner for $s=2$, lower right-hand corner for $s=3$). Plasmons with $s=1$ can be considered as dipole plasmon modes, $s=2, 3,...$ as multipole plasmon modes.
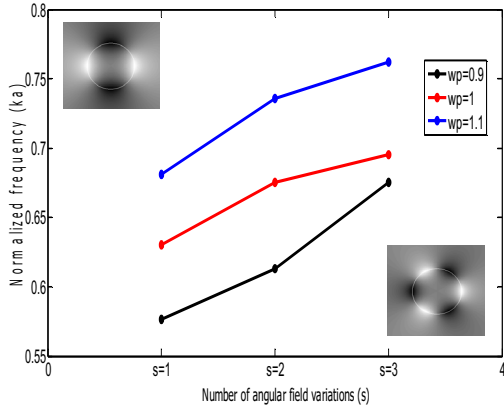

Figure 1. Dependence of the eigenfrequency on the number of angular field variations for different values of the normalized plasma frequency w_p.
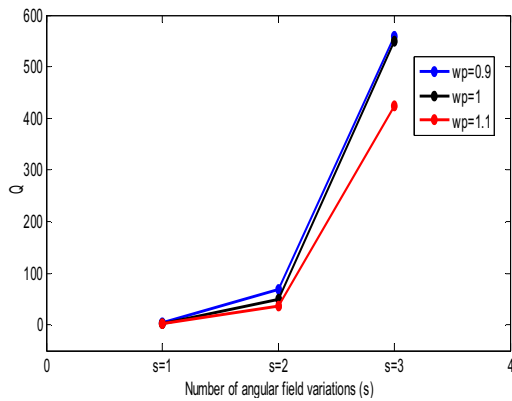

Figure 2. Dependence of the Q-factor on the number of angular field variations for isolated plasma cylinder for different values of the normalized plasma frequency w_p ($s=1, 2, 3$).

Figure 2 shows the dependence of Q-factor on the number of angular field variations for different values of the normalized plasma frequency w_p. It shows the increase of Q-factor with increasing of s for different values of the normalized plasma frequency w_p.

For the case of two coupled plasma cylinders the structure has two symmetry axes that causes four classes of excited plasmons with different symmetry: EE (even symmetry with respect to x and y axes), EO (x – even; y - odd), OE (x – odd; y - even), OO (x – odd; y - odd). Consequently the plasmonic

modes of the coupled plasma cylinders can be viewed as symmetric and antisymmetric combinations of plasmons of isolated cylinder.
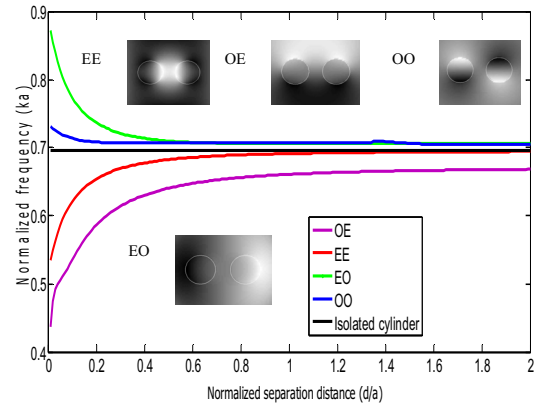

Figure 3. The normalized frequency versus the normalized separation distance between the two coupled plasma cylinders for EE, OE, EO, OO plasmons ($s=1$) and for isolated cylinder ($s=1$).
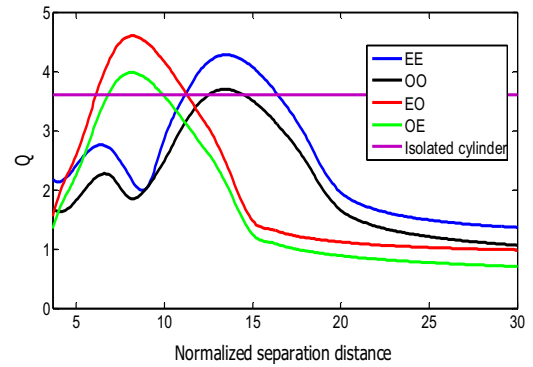

Figure 4. Q-factor for two coupled plasma cylinders ($s=1$, $w_p=1$) for EE, OE, EO, OO plasmons and for isolated cylinder ($s=1$)

Figure 3 demonstrates the real values of the eigenfrequencies of the EE, EO, OE, OO plasmons ($s=1$) for two coupled plasma cylinders ($w_p=1$) and for isolated cylinder ($s=1$). It is clearly seen that for distant cylinders eigenfrequencies are nearly identical for all four symmetry classes. As separation distance d becomes smaller, the frequency shift of the coupled plasmons becomes much stronger. The near-field distributions of different plasmons ($s=1$) of two plasma cylinders are shown in the insets in Fig. 3.

The Q-factor of dipole plasmons in two coupled plasma cylinders ($s=1$) is shown if Fig. 4. We examined the range of normalized separation distance from 0 to 30. For distant plasma cylinders Q of coupled plasmonic modes is evidently smaller than Q factor of corresponding plasmons of the isolated cylinder. Peaks of Q are observable for the case when separation distance tends to the wavelength.

Adding one more plasma cylinder does not alter the number of the symmetry axes of the structure however bonding and antibonding combinations of the plasmons can be excited. Figure 5 demonstrates the near-field distributions of different plasmons of three coupled plasma cylinders for different number of angular field variations and for different values of the normalized separation distance between the coupled cylinders.

| a) EOa, | b) EOb, | c) EOb, |
| $s=1$, $d/a=0.5$. | $s=1$, $d/a=0.5$. | $s=2$, $d/a=1$. |

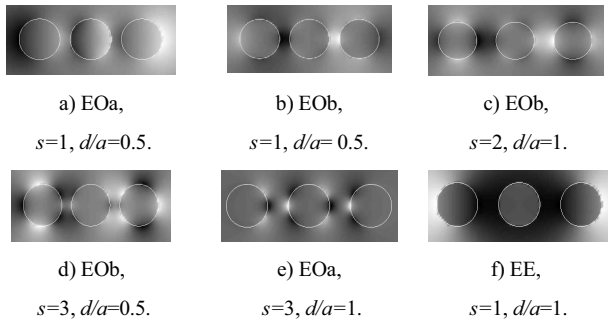| d) EOb, | e) EOa, | f) EE, |
| $s=3$, $d/a=0.5$. | $s=3$, $d/a=1$. | $s=1$, $d/a=1$. |

Figure 5.   The near-field distributions of different plasmons of three coupled plasma cylinders for different number of angular field variations.

Figures 6 and 7 show the real values of the eigenfrequencies of the different plasmons in a chain of three coupled cylinders: $s=1$ (dipole modes) and $s=2$ (quadrupole modes), respectively. We see the appearance of bonding and antibonding modes in EO and OE symmetry classes for dipole modes ($s=1$). However for quadrupole modes ($s=2$) we observe reverse situation that means appearance of bonding and antibonding modes in EE and OO classes. It can be seen that the upward shift in frequency is much faster than downward shift for both dipole and quadrupole modes (see Figs. 6 and 7). We compare the Q-factors of dipole and quadrupole plasmons in chain of three plasma cylinders in Figs. 8 and 9. The growth of Q-factors for certain separation distances is observable. Dramatic enhancement in Q for quadrupole modes is evident.
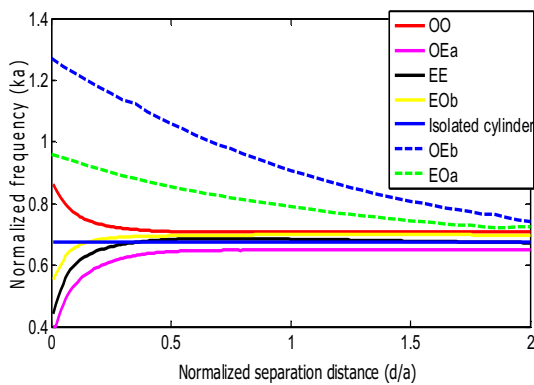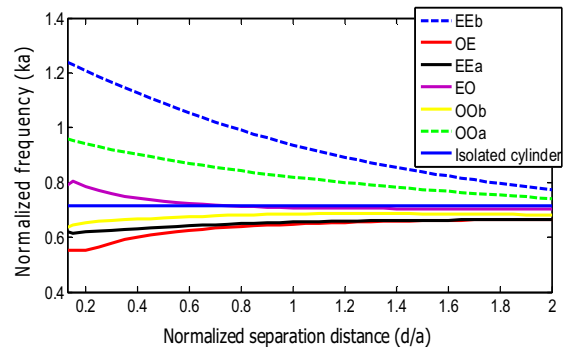

Figure 6.   The normalized frequency versus the normalized separation distance between the three coupled plasma cylinders for different plasmons ($s=1$) and for isolated cylinder ($s=1$).

In a linear chain of four coupled cylinders bonding and antibonding modes appear in each symmetry class. We have to mention the total number of excided plasmons for each value of s twice greater that number of cylinders in a chain.

Figure 7.   The normalized frequency versus the normalized separation distance between the three coupled plasma cylinders for different plasmons ($s=2$) and for isolated cylinder ($s=2$).
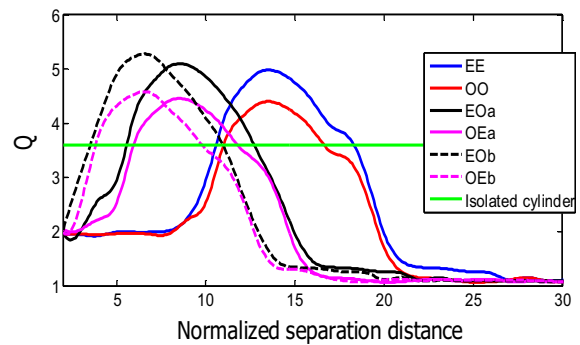

Figure 8.   Q-factor for three coupled plasma cylinders ($s=1$, $w_p=1$) for different plasmons and for isolated cylinder ($s=1$).
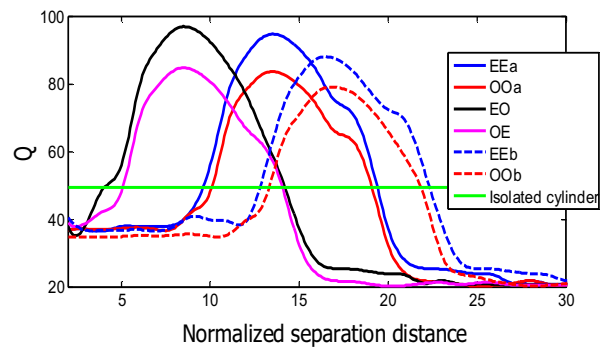

Figure 9.   Q-factor for three coupled plasma cylinders ($s=2$, $w_p=1$) for different plasmons and for isolated cylinder ($s=2$).

Figure 10 presents eigenfrequencies of coupled EE dipole plasmonic modes in a chain of plasma cylinders. It is seen that for large separation distances between cylinders all modes converge to plasmon modes of an isolated plasma cylinder. With decreasing of the separation distance we observe up-shifting of the frequency for bonding modes and down-shifting for antibonding modes.
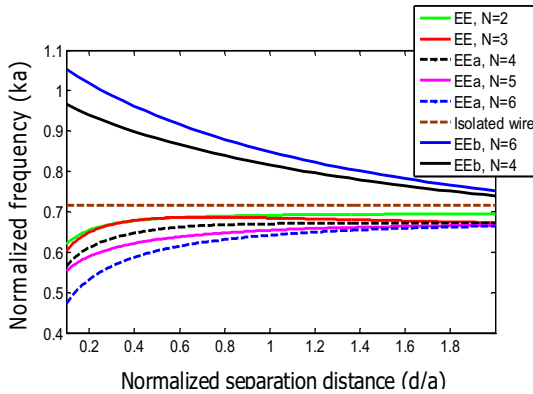

Figure 10. The normalized frequency versus the normalized separation distance between the coupled plasma cylinders in a chain on N cylinders for EE plasmon ($s=1$) and for isolated cylinder ($s=1$).
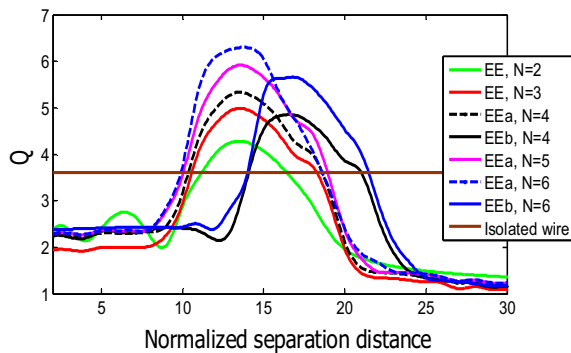

Figure 11. Q-factor for chain of N coupled plasma cylinders ($s=1$, $w_p=1$) for EE plasmons and for isolated cylinder ($s=1$).

Figure 11 shows the Q factor of a variety of EE plasmons. We see the growing of Q with increasing the number of cylinders in a chain, besides the Q for antibonding plasmons exceed those for bonding ones.

IV. CONCLUSIONS

The eigenfrequencies of the coupled cylinders filled with negative permittivity plasma have been analyzed. It has been shown that individual plasmons of isolated column interact and form symmetric and antisymmetric plasmonic coupled modes of different types. Accurate analysis of the influence of the coupling of plasma cylinders on their spectrum of different plasmon resonances is presented.

REFERENCES

[1] A. Zayats, I. Smolyaninov, "Near-field photonics: surface plasmon polaritons and localized surface plasmons," Journal of Optics A: Pure and Applied Optics, vol. 5, 2003, pp. 16-50.
[2] W. Barnes, A. Dereux, and T. Ebbesen, "Surface plasmon subwavelength optics," Nature, 424, 2003, pp. 824-830.
[3] S. Bozhevolnyi, V. Volkov, E. Devaux, J. Laluet, and T. Ebbesen, "Channel plasmon subwavelength waveguide components including interferometers and ring resonators," Nature, vol. 440, 2006, pp.508-511.
[4] Y. Zhao, Y. Hao, "Finite-difference time-domain study of guided modes in nano-plasmonic waveguides," IEEE Trans. Antennas Propag., vol. 55, 2007, pp. 3070-3077.
[5] H. R. Stuart, A. Pidwerbetsky, "Electrically small antenna elements using negative permittivity resonators," IEEE Trans. Antennas and Propagation, vol. 54, 2006, pp. 1644-1653.
[6] J. li and N. Engheta, "Ultracompact sub-wavelength plasmonic cavity resonator on a nanowire," Phys. Rev. B, vol. 74, 2006, 115125.
[7] P. Muhlschlegel, H. Eisler, O. Martin, B. Hecht, D. Pohl, "Resonant optical antennas," Science, vol. 308, 2005, pp. 1607-1609.
[8] L. Novotny and N. Hulst, "Antennas for light," Nature Photonics, vol. 5, 2011, pp. 83-90.
[9] N. Bonod, A. Devilez, B. Rolly, S. Bidault, and B. Stout, "Ultracompact and unidirectional metallic antennas," Phys. Rev. B, 82, 2010, 115429.
[10] K. Kneipp, Y. Wang, H. Kneipp, L. Perelman, I. Itzkan, R. Dasari, and M. Feld, "Single molecule detection using surface-enhanced Raman scattering (SERS)," Phys. Rev. Lett., vol. 78, 1997, pp. 1667–1670.
[11] J. Bahns, A. Imre, V. Vlasko-Vlasov, J. Pearson, J. M. Hiller, L. H. Chen, and U. Welp, "Enhanced Raman scattering from focused surface plasmons," Appl. Phys. Lett., vol. 91, 2007, 081104.
[12] J. Weiner, "The physics of light transmission through subwavelength apertures and aperture arrays," Reports on Progress in Physics, vol. 72, 2009, 064401.
[13] T. Thio, K. Pellerin, R. Linke, H.Lezec, T. Ebbesen, "Enhanced light transmission through a single subwavelength aperture," Optics Letters, vol. 26, 2001, pp.1972-1974.
[14] I. Smolyaninov, J. Elliott, A. Zayats, and C. C. Davis, "Far-field optical microscopy with a nanometer-scale resolution based on the in-plane image magnification by Surface Plasmon Polaritons," Phys. Rev. Lett., vol. 94, 2005, 057401.
[15] E. Ozbay, "Plasmonics: merging photonics and electronics at nanoscale dimension," Science, vol. 311, 2006, pp. 189-193.
[16] K. Kim, S.J. Yoon, D. Kim, "Nanowire-based enhancement of localized surface plasmon resonance for highly sensitive detection: a theoretical study," Optics Express, vol. 14, no. 25, 2006, pp. 12419-12431.
[17] D. Fedyanin, A. Arsenin, "Transmission of surface plasmon polaritons through a nanowire array: mechano-optical modulation and motion sensing," Optics Express, vol. 18, no. 19, 2010, pp. 20115-20124.
[18] G. Dice, S. Mujumdar, and A. Elezzabi, "Plasmonically enhanced diffusive and subdiffusive metal nanoparticle-dye random laser," Appl. Phys. Lett., vol. 86, 2005, 131105.
[19] M. Noginov, G. Zhu, A. Belgrave, R. Bakker, V. Shalaev, E. Narimanov, S. Stout, E. Herz, T. Suteewong, and Wiesner, "Demonstration of a spaser-based nanolaser," Nature, vol. 460, 2009, pp. 1110-1113.